# Sterol regulatory element binding transcription factor 1 promotes proliferation and migration in head and neck squamous cell carcinoma

Ming Tan [1] , Xiaoyu Lin [1] , Huiying Chen [1] , Wanli Ye [1] , Jianqi Yi [1] , Chao Li [1] , Jinlan Liu [1] , Jiping Su [Corresp. 1]

[1] First Affiliated Hospital of Guangxi Medical University, Nanning, nanning, china

Corresponding Author: Jiping Su
Email address: ymsu2@126.com

**Background** Sterol-regulatory element-binding protein 1 (SREBP1) is a transcription factor involved in lipid metabolism that is encoded by sterol regulatory element binding transcription factor 1(SREBF1). SREBP1 overexpression is associated with the progression of several human tumors; however, the role of SREBP1 in head and neck squamous cell carcinoma (HNSC) remains unclear. **Methods** SREBF1 expression in pan-cancer was analyzed using the Cancer Genome Atlas (TCGA) and Genotype-Tissue Expression (GTEx) data, and the association between SREBF1 expression and clinical characteristics of HNSC patients was examined using the UALCAN database. Enrichment analysis of SREBF1-related genes was performed using the Cluster Profiler R package. TCGA database was used to investigate the relationship between immune cell infiltration and SREBF1 expression. CCK-8, flow cytometry, and wound healing assays were performed to investigate the effect of SREBF1 knockdown on the proliferation and migration of HNSC cells. **Results** SREBF1 was significantly upregulated in several tumor tissues, including HNSC, and SREBF1 overexpression was positively correlated with sample type, cancer stage, tumor grade, and lymph node stage in HNSC patients. Gene enrichment analysis revealed that SREBF1 is associated with DNA replication and homologous recombination. SREBF1 upregulation was positively correlated with the infiltration of cytotoxic cells, B cells, T cells, T helper cells, and NK CD56 bright cells in HNSC. Knockdown of SREBF1 inhibited the proliferation and migration of HNSC cells (Hep2 and TU212) and induced apoptosis by downregulating the expression of steroidogenic acute regulatory protein-related lipid transfer 4(STARD4). **Conclusions** SREBF1 may promote HNSC proliferation, migration and inhibit apoptosis by upregulating STARD4 and affecting the level of immune cell infiltration.

1 Sterol regulatory element binding transcription factor 1 promotes proliferation and

2 migration in head and neck squamous cell carcinoma

3 Ming Tan1   Xiaoyu Lin1   Huiying Chen1   Wanli Ye1   Jianqi Yi1   Chao Li1   Jinlan Liu1   Jiping Su2

5 ¹ Department of Otolaryngology-Head and Neck Surgery, First Affiliated Hospital of Guangxi Medical

6 University, Nanning, 530021, Guangxi, China.

7 ² Department of Otolaryngology-Head and Neck Surgery, First Affiliated Hospital of Guangxi Medical

8 University, Nanning, 530021, Guangxi, China. ymsu2@126.com.

10 **Abstract**

11 **Background**

12 Sterol-regulatory element-binding protein 1 (SREBP1) is a transcription factor

13 involved in lipid metabolism that is encoded by sterol regulatory element binding

14 transcription factor 1 ( SREBF1). SREBP1 overexpression is associated with the

15 progression of several human tumors; however, the role of SREBP1 in head and

16 neck squamous cell carcinoma (HNSC) remains unclear.

17 **Methods**

18 SREBF1 expression in pan-cancer was analyzed using the Cancer Genome Atlas

19 (TCGA) and Genotype-Tissue Expression (GTEx) data, and the association

20 between SREBF1 expression and clinical characteristics of HNSC patients was

21 examined using the UALCAN database. Enrichment analysis of SREBF1-related

22  genes was performed using the Cluster Profiler R package. TCGA database was

23  used to investigate the relationship between immune cell infiltration and SREBF1

24  expression. CCK-8, flow cytometry, and wound healing assays were performed to

25  investigate the effect of SREBF1 knockdown on the proliferation and migration of

26  HNSC cells.

27  Results

28  SREBF1 was significantly upregulated in several tumor tissues, including HNSC,

29  and SREBF1 overexpression was positively correlated with sample type, cancer

30  stage, tumor grade, and lymph node stage in HNSC patients. Gene enrichment

31  analysis revealed that SREBF1 is associated with DNA replication and

32  homologous recombination. SREBF1 upregulation was positively correlated with

33  the infiltration of cytotoxic cells, B cells, T cells, T helper cells, and NK CD56

34  bright cells in HNSC. Knockdown of SREBF1 inhibited the proliferation and

35  migration of HNSC cells (Hep2 and TU212) and induced apoptosis by

36  downregulating the expression of steroidogenic acute regulatory protein-related

37  lipid transfer 4(STARD4).

38  Conclusions

39  SREBF1 may promote HNSC proliferation, migration and inhibit apoptosis by

40  upregulating STARD4 and affecting the level of immune cell infiltration.

41  Keywords: SREBF1, HNSC, cell proliferation, migration, immune infiltration

## 1. Introduction

42

43 Head and neck squamous cell carcinoma (HNSC) is the 7th most common

44 malignancy worldwide and one of the most aggressive tumors(Ahmad Kiadaliri et

45 al. 2013; Torre et al. 2015). More than 830,000 cases of HNSC are diagnosed

46 worldwide each year, and over 430,000 people die from the disease(Cramer et al.

47 2019). Local recurrence and distant metastasis are the main causes of death in

48 patients with HNSC. Although the diagnosis and treatment of HNSC have made

49 progress in the past decades, the 5-year overall survival rates have not improved

50 significantly(Yang et al. 2019). Despite more and more oncogenes having been

51 identified with the continuous progress of transcriptome research and high-

52 throughput sequencing technology, effective molecular biomarkers for detecting

53 early HNSC and monitoring disease progression are lacking.

54 Growing evidence suggests that lipid metabolism reprogramming is ubiquitous in

55 tumor cells(Schulze & Harris 2012). Abnormal lipid metabolism promotes the

56 malignant biological behavior of tumors (Luo et al. 2017; Tudek et al. 2017). In

57 tumor cells, glucose and glutamine contribute to the synthesis of lipids in response

58 to the PI3K/Akt (phosphatidylinositol-3-kinase/protein kinase B) signaling

59 pathway and a series of key enzymes(Cheng et al. 2018). Sterol-regulatory

60 element-binding protein 1 (SREBP1), encoded by the sterol regulatory element

61 binding transcription factor 1 ( SREBF1) gene, is an important nuclear

62 transcription factor involved in lipid synthesis. SREBP1 is synthesized into

63 inactive precursors on the endoplasmic reticulum and then transported to the Golgi

64 apparatus where it is activated by proteases. Mature SREBP1 promotes lipid

65 synthesis by activating the expression of downstream target genes(Han et al. 2015).

66 Abnormal expression of SREBP1 is correlated with tumor progression in

67 differentiated thyroid cancer, esophageal squamous cell carcinoma, glioblastoma,

68 and ovarian cancer(Cheng et al. 2015; Huang et al. 2019; Koizume et al. 2019; Li

69 et al. 2020b). SREBP1 is regulated by the PI3K/Akt oncogenic signaling

70 pathway(Yi et al. 2020), which is activated in more than 90% of HNSC(Marquard

71 & Jucker 2020). Tumor immune cell infiltration plays an important role in tumor

72 recurrence, metastasis, and immunotherapy(Jiang et al. 2018; Zeng et al. 2018).

73 Immune cells are an important part of the tumor microenvironment in

74 HNSC(Puram et al. 2017). However, there are no studies investigating the role of

75 SREBF1 in the proliferation and immune infiltration of HNSC.

76 In this study, we will perform a comprehensive analysis of SREBF1 expression

77 using multiple publicly available gene expression databases and investigate the

78 correlation of SREBF1 expression in HNSC with sample type, cancer stage, lymph

79 node status, and tumor grade. In addition, we will validate the expression of

80 SREBF1 in HNSC and further investigate the effect of the knockdown of SREBF1

81 on the proliferation and migration of HNSC. This study provides a new idea for the

82 targeting of SREBF1 in HNSC.

83 2.Materials and Methods

84 2.1 Gene expression analysis data

85 We combined the Cancer Genome Atlas (TCGA) and Genotype-Tissue Expression

86 (GTEx) databases to analyze the differential expression of SREBF1 in pan-cancer

87 and then analyzed the expression of SREBF1 and steroidogenic acute regulatory

88 protein-related lipid transfer 4(STARD4) in HNSC in TCGA paired and unpaired

89 samples. The UALCAN database was then used to analyze the correlation of

90 SREBF1 and STARD4 expression with sample type, tumor stage, lymph node

91 stage, and tumor grade.

92 **2.2   Correlation and enrichment analysis**

93 We performed an enrichment analysis of genes significantly associated with

94 SREBF1 expression in HNSC according to the TCGA database to understand the

95 function of SREBF1. For enrichment analysis, the Cluster Profiler package in R

96 software (version 3.6.3) was used.

97 **2.3   Immune cell infiltration analysis**

98 We used 24 kinds of immune cell markers to distinguish different immune cells

99 according to a previous study(Bindea et al. 2013), and the correlation between

100 immune cell infiltration and SREBF1 expression was analyzed using single sample

101 gene enrichment analysis (ssGSEA) (Hanzelmann et al. 2013).

102 **2.4   Cell culture and transfection**

103 The Human HNSC cell lines Hep2 was donated by Professor Zhang zhe from the

104 Nasopharyngeal Cancer Laboratory of Guangxi Medical University, and the SAS

105 and SCC-9 were donated by Prof. Li Ping from Guangxi Medical University.

106 TU212 was purchased from Beijing Zhongkezhijian Biotechnology Co., Ltd. FaDu

107 and the normal human HOK were purchased from Shanghai WHELAB Bioscience

108 Co., Ltd. Hep2 cells were cultured in DMEM with high glucose containing 10%

109 fetal bovine serum (FBS, Gibco, USA, 10091148) and 1% streptomycin and

110 penicillin (Sigma, USA, P1400). The remaining cells were maintained according to

111 the manufacturer's protocol, and all cells were incubated at 37°C, with 5% $CO_2$.

112 SREBF1-siRNA(Sense 5' -GCCUGACCAUCUGUGAGAATT-3 ', antisense 5' -

113 UUCUCACAGAUGGUCAGGCTT3 '), Negative control SREBF1 - siNC ( sense

114 5'- UUCUCCGAACGUGUCACGUTT - 3', antisense 5'-

115 ACGUGACACGUUCGGAGAATT -3' ) and GP-transfect-Mate reagent were

116 purchased from Shanghai GenePharma Co., Ltd (Shanghai, China, G04008). Hep2

117 and TU212 cells were inoculated on 6-well plates, the OPTI-MEM (Thermo

118 Scientific, USA, Cat. No. 31985070) mixture with 7.5μl of GP-transfect-Mate

119 transfection reagent and the OPTI-MEM mixture with 8.5μl of SREBF1-

120 siRNA/SREBF1-siNC were mixed well. Transfection was carried out after 15 min

121 at room temperature. The transfected cells were used for the next experiment.

122 **2.5  RNA Extraction and Real-Time RT-PCR(RT-qPCR)**

123 Total RNA was extracted from cultured cells using TRIzol reagent (Invitrogen,

124 USA, 15596026), and reverse transcription was performed using a reverse

125 transcription kit (TransGen Biotech, China, AT311). Reverse transcription-

126 quantitative (RT-q)PCR was performed using the SYBR Green PCR kit

127 (Invitrogen, USA, A25741). SREBF1 primers: forward 5'-

128 ACAGTGACTTCCCTGGCCTAT-3' and reverse 5' -

129 GCATGGACGGGTACATCTTCAA-3 '. STARD4 primers: forward 5'-

130 TCCCTGTGGTTGGTTTTGTGTTCC-3' and reverse 5' -

131 TGGCTGTATCTACCGCAGACTGAG-3 '. GAPDH primers: forward 5' -

132 CAGGAGGCATTGCTGATGAT-3 'and reverse 5' -

133 GAAGGCTGGGGCTCATTT-3'. GAPDH was used as an internal reference. The

134 expression levels of mRNA were analyzed by the $2^{-\Delta\Delta CT}$ method. Each experiment

135 was repeated at least three times.

136 **2.6 Western Blotting**

137 Total cellular proteins were extracted from cultured cells($1.2\times10^6$/well )using cell

138 lysate (RIPA buffer, protease inhibitor, and phosphatase inhibitor, P0013B), and

139 the extracted proteins were mixed with 5× SDS-PAGE protein loading solution at a

140 ratio of 4:1 and then heated to degeneration sufficiently. After running the protein

141 samples(80 μg) on SDS-PAGE gels, they were transferred to PVDF membranes,

142 closed with 5% skim milk, and then mixed with the primary antibodies indicated(

143 SREBF1 mouse monoclonal antibody (1:1000, Proteintech, Wuhan, China, Cat

144 No. 66875-1-Ig), STARD4 antibody (1:1000, Abcam, ab202060), GAPDH

145 antibody(1:20000, Proteintech, Wuhan, China, Cat No. 60004-1-Ig))overnight at

146 4°C, and then the PVDF membrane was scanned using infrared scanning

147 equipment after incubation with secondary antibodies(Anti-mouse IgG (H+L),

148 1:15000, CST, 5470), Anti-rabbit IgG (H+L), 1:15000, CST, 5366). ImageJ

149 software was used to analyze the relative expression of target proteins in

150 membranes.

151 2.7 CCK-8 (Cell counting kit - 8) Assay

152 For this study, CCK-8 assays (Dojindo Cell counting tool test - 8th Edition, Japan,

153 JE603) were used. The transfected cells were plated in 96-well plates at a

154 concentration of 3000 cells per well. 10μ L CCK-8 solution was added to each well

155 at 24h, 48h, 72h, and 96h, then the cells were incubated at 37°C for 3 h. A 450-nm

156 absorbance wavelength was used to measure the OD value of each well.

157 2.8 Wound healing assay

158 The transfected cells were plated in a 6-well plate with ibidi Culture-Insert, and

159 incubated in the incubator for 24 hours. After the Culture-Insert was removed, the

160 cells were washed with PBS and incubated with 2% FBS. The cell migration status

161 was recorded at 0h and 24h with the optical microscope.

162 **2.9 Flow Cytometric Assessment**

163 Cells were collected 24 hours after transfection, washed twice with pre-chilled

164  1×PBS, and resuspended to a density of approximately $1×10^6$ cells/ml. 100 μL of

165  the cell suspension was transferred to a 1.5 ml EP tube, and 5 μL of FITC Annexin

166  V, and 5 μL of PI reagent (BD Biosciences, San Diego, CA, 556547) were added

167  and mixed well. Incubate for 15 minutes at room temperature in the dark. Flow

168  cytometry was then performed.

169  2.10 Statistical analysis

170  Data were expressed as the mean ± standard deviation (SD) and analyzed using

171  SPSS 26.0 (SPSS, Chicago, IL, USA). The Shapiro-Wilk test was used to

172  check the normality of the data. T test was used for samples that met the

173  normality test, and the Wilcoxon rank sum test was used for samples that

174  did not meet the normality test. $P < 0.05$ was considered statistically

175  significant.

176  3 Results

177  3.1 Expression analysis of SREBF1 in pan-cancer

178  Analysis of the TCGA and GTEx databases revealed that SREBF1 expression is

179  significantly increased in bladder urothelial carcinoma (BLCA) ($P < 0.01$), breast

180  invasive carcinoma (BRCA), lymphoid neoplasm diffuse large B-cell lymphoma

181  (DLBC), esophageal carcinoma (ESCA), HNSC, kidney chromophobe (KICH),

182  kidney renal clear cell carcinoma (KIRC), kidney renal papillary cell carcinoma

183  (KIRP), brain lower grade glioma (LGG), pancreatic adenocarcinoma (PAAD),

184  stomach adenocarcinoma (STAD), and thymoma (THYM) ($P < 0.001$) tumors

185 compared with adjacent normal tissues(Figure 1A). Further analysis of the TCGA

186 database revealed that SREBF1 and STARD4 expression is significantly higher in

187 HNSC tumor tissues than in adjacent normal tissues(Figure 1B-E).

188

189 Figure 1. SREBF1 expression in human pan-cancers. (A) TCGA and GTEx databases provide

190 information on SREBF1 expression in tumors and adjacent normal tissues, HNSC (Normal=44,

191 Tumor=520). (B-C) Expression of SREBF1 and STARD4 in adjacent normal tissues and tumors

192 in HNSC( Normal=44, Tumor=502) from unpaired samples in TCGA. (D-E) Expression of

193 SREBF1 and STARD4 in tumor and adjacent normal tissues in HNSC (Normal=43, Tumor=43)

194 from paired samples in TCGA. TPM (transcripts per million reads), Data are shown as the mean

195 ± SD. *P < 0.05, **P < 0.01, ***P < 0.001.

196 3.2 SREBF1 expression and HNSC clinicopathology

197 Analysis of the UALCAN database indicated that the expression of SREBF1 and

198 STARD4 correlated with sample type, tumor stage, lymph node stage, and tumor

199 grade. As shown in Figure 2A+B, the expressions of SREBF1 and STARD4 were

200 significantly higher in HNSC tumor tissues than in adjacent normal tissues (P <

201 0.001). Figure 2C+D shows that the expressions of SREBF1 and STARD4 were

202 significantly higher in mid to late-stage than in early-stage tumors. During cancer

203 progression, the expressions of SREBF1 and STARD4 were significantly higher in

204 the lymph node metastatic stage than in normal tissues (Figure 2E+F). Analyses of

205 SREBF1 and STARD4 expressions with tumor grade indicated that their

206  expressions increased significantly with increasing tumor grade (Figure 2G+H).

207  These results suggest that SREBF1 and STARD4 play important roles in the

208  pathogenesis of HNSC.

209

210  Figure 2. Correlation of SREBF1 and STARD4 mRNA expression with clinicopathological

211  parameters in HNSC patients from the UALCAN database. (A+B)Type of sample

212  (normal/primary tumor). (C+D)Cancer stage (stage1,2, 3,and4). (E+F)Lymph node stage

213  (N0,1,2,and3). (G+H)Tumor grade (Grades 1, 2, 3, and 4). N, normal; P, primary tumor; S1,

214  stage 1; S2, stage 2; S3, stage 3; S4, stage 4.G1, Grade1; G2, Grade2; G3, Grade3; G4, Grade4.

215  3.3 Enrichment analysis of SREBF1-related genes

216  To investigate the potential mechanism of SREBF1 in the development of HNSC,

217  we used the TCGA database screening SREBF1 expression-related mRNAs in

218  HNSC (according to a study in the past p_spearman < 0.001 and | cor_spearman | >

219  0.4(Chen et al. 2020)), then analyzed the potential function of these genes. The

220  heat map shows the top 50 genes (Figure 3), and the Kyoto Encyclopedia of Genes

221  and Genomes (KEGG) enrichment analysis revealed that SREBF1 expression was

222  associated with Fanconi anemia pathway, DNA replication, and homologous

223  recombination (Figure 4A). Gene ontology (GO) analysis revealed that the three

224  most enriched terms in biological process ontology were DNA replication,

225  chromosome segregation, and DNA conformation change. In the cellular

226  component ontology, the three most enriched terms were chromosomal region,

227   nuclear chromatin, and spindle. For molecular functional ontology, the top three

228   terms were catalytic activity, acting on DNA, histone binding, and single-stranded

229   DNA binding (Figure 4B-D). These results indicate that overexpression of

230   SREBF1 is associated with cell proliferation and that overexpression of SREBF1

231   in HNSC is associated with tumor progression.

232

233   Figure 3. Analysis of SREBF1-related genes. The top 50 genes positively associated with

234   SREBF1 expression are shown in the heat map. The data were normalized by the Z-score

235   normalization method.

236

237   Figure 4. Enrichment analysis of SREBF1-related genes in HNSC. (A) KEGG pathways of genes

238   significantly associated with SREBF1. (B-D) Gene ontology terms are significantly associated

239   with SREBF1 [including biological processes (B), cell components (C), and molecular function

240   (D)].

241   3. 4  SREBF1 expression is associated with immune cell infiltration

242   Immune cells that infiltrate tumors play a critical role in cancer

243   progression(Fridman et al. 2011; Wu & Dai 2017). We evaluated the correlation

244   between SREBF1 expression in HNSC and the infiltration of 24 immune cells. The

245   results showed that infiltration of    NK CD56 bright cells and T helper cells was

246   higher in the high SREBF1 expression group than in the low SREBF1 expression

247   group (Figure 5A). The expression of    SREBF1 was significantly and positively

248   correlated with the infiltration of NK CD56 bright cells and T helper cells(Figure

249   5B). This suggested that high expression of SREBF1 in HNSC caused increased

250   enrichment of  NK CD56 bright cells and T helper cells, indicating that

251   overexpression of SREBF1 was associated with immune activation in HNSC.

252

253   Figure 5. SREBF1 expression and immune cell infiltration in HNSC are correlated. (A)

254   Comparison of immune cell infiltration levels between SREBF1 differentially expressed groups

255   in TCGA cohort of HNSC. (B) Correlation between SREBF1 and immune cell infiltration levels;

256   red represents a positive correlation, green represents a negative correlation, and color shades

257   represent the strength of the correlation. The data are presented as the mean ± standard deviation.

258   *P < 0.05, **P < 0.01, ***P < 0.001. ns, not significant.

259   3. 5  Knockdown of SREBF1 inhibits the proliferation and motility of HNSC cells

260   To assess the mechanism underlying the role of SREBF1 in HNSC progression, the

261   target genes downstream of SREBF1 were first queried in the Chip-Atlas database

262   (https://chip-atlas.org/). STARD4 is an important cholesterol transporter protein

263   involved in the regulation of intracellular cholesterol homeostasis. Intracellular

264   STARD4 binds free cholesterol to promote the formation of cholesteryl

265   esters(Rodriguez-Agudo et al. 2008). Moreover, analysis in the TCGA database

266   revealed a significant positive correlation between STARD4 and SREBF1 in

267   HNSC(r=0.239, P < 0.001, Supplementary Figure 1). Cellular assays showed that the

268   expression of SREBF1 and STARD4 was significantly higher in HNSC cell lines

269     than in normal human HOK cells (Figure 6A). We then knocked down the

270     expression of endogenous SREBF1 in HNSC cells (Hep2 and TU212) by RNA

271     interference, RT-qPCR detected that SREBF1 was down-regulated along with

272     STARD4 (Figure 6B). The results of the Western blot assay were consistent with

273     the results of the RT-qPCR assay (Figure 6C). Next, we assessed cell proliferation

274     using the CCK8 assay and found that the knockdown of SREBF1 significantly

275     reduced the proliferation ability of HNSC cells (Hep2 and TU212) (Figure 6D-E).

276     Knockdown of SREBF1 significantly increased apoptosis in HNSC cells (Hep2

277     and TU212) as shown by flow cytometry (Figure 6F-G). Silencing of SREBF1

278     significantly decreased the migration ability of HNSC cells (Hep2 and TU212) as

279     shown by wound healing assays (Figure 6H). Taken together, these results

280     suggested that SREBF1 may promote the proliferation and migration of HNSC

281     through the upregulation of STARD4.

282

283     Figure 6. Knockdown of SREBF1 inhibited the proliferation and migration of HNSC cells. (A)

284     Expression levels of SREBF1 mRNA and STARD4 mRNA were measured in HNSC cells by

285     RT-qPCR. (B) SREBF1 was knocked down by RNA interference, and the levels of SREBF1 and

286     STARD were assessed by RT-qPCR. (C) Western blot analysis of SREBF1 and STARD4 levels.

287     (D-G) CCK-8 assay and flow cytometric assessment were used to detect HNSC cell growth. (H)

288     A wound-healing assay was used to detect the capacity of HNSC cells to migrate (original

289     magnification ×100). The data are presented as the mean ± SD. *P < 0.05, **P < 0.01, ***P <

290   0.001, ****P < 0.0001.

## 4 Discussion

The five-year overall survival rate of HNSC has been hovering around 50%(Thariat et al. 2015), so it is urgent to further understand the pathogenesis of this kind of disease.  Lipid metabolism in malignant tumors has become the focus of research. Reprogramming of lipid metabolism is one of the hallmarks of malignancy (Cheng et al. 2018). Lipids not only serve as important components of biological membranes but also play a critical role in cellular signal transduction processes (Rohrig & Schulze 2016). SREBP1 is a key transcription factor involved in the regulation of lipid metabolism, and it plays a regulatory role in various human metabolic diseases; it also serves as a hub linking oncogenic signaling and tumor metabolism(Guo et al. 2014). SREBP1 expression is significantly increased in tumors and plays an integral role in tumor progression (Gao et al. 2019; Zhou et al. 2019; Zhou et al. 2020). SREBP1 expression is significantly higher in breast cancer than in adjacent normal tissues, and knockdown of SREBP1 inhibits the proliferation, migration, and invasion of tumor cells(Zhang et al. 2019). SREBP1 is overexpressed in renal clear cell carcinoma, and silencing SREBP1 inhibits tumor progression through the NF-κB signaling pathway(Yang et al. 2018). Knockdown of SREBP1 in colon cancer inhibits tumor growth by altering cellular metabolism through the downregulation of genes related to lipid metabolism(Wen et al. 2018).Upregulation of SREBP1 expression in human hepatocellular carcinoma

311   correlates with a poor prognosis of patients(Li et al. 2014). This suggests that

312   SREBP1 plays an oncogenic role in the progression of several human cancers.

313   Novel inhibitors of SREBP1 can significantly inhibit the growth of hepatocellular

314   carcinoma and prostate cancer(Meng et al. 2021; Singh et al. 2019). These results

315   suggest that SREBP1 is a novel molecular target in cancer. However, the

316   expression of SREBF1 in human cancers and its potential mechanism of action

317   remain unclear. In the present study, we used the TCGA and GTEx databases to

318   analyze SREBF1 expression in human pan-cancer and found that SREBF1 was

319   significantly upregulated in 12 cancers, including BLCA, BRCA, DLBC, ESCA,

320   HNSC, KICH, KIRC, KIRP, LGG, PAAD, STAD, and THYM. However, the

321   expression of SREBF1 was reduced in other tumors, such as adrenocortical

322   carcinoma(ACC), colon adenocarcinoma( COAD), glioblastoma

323   multiforme(GBM), acute myeloid leukemia (LAML), liver hepatocellular

324   carcinoma(LIHC), lung adenocarcinoma(LUAD), ovarian serous

325   cystadenocarcinoma( OV), pheochromocytoma and paraganglioma(PCPG), rectum

326   adenocarcinoma(READ), skin cutaneous melanoma (SKCM), testicular germ cell

327   tumors(TGCT), thyroid carcinoma(THCA), and uterine carcinosarcoma (UCS).

328   This suggests that SREBF1 plays an important role in the progression of many

329   tumors, the role of SREBF1 in low-expressing tumors may need to be investigated

330   in depth. Previous studies have shown that Fatostatin, an inhibitor of SREBP1, can

331   reduce the activity of cancer cells (HeLa, SH-SY5Y, and U2OS) and normal cells

332 (RPE and MEFs), but has a more pronounced effect on cancer cell viability (~ 10-

333 20% cell viability vs ~ 50-62% cell viability)(Gholkar et al. 2016; Ma et al.

334 2021).These findings suggest that the use of SREBP1 inhibitors in the targeted

335 treatment of cancers with high SREBP1 expression may also interfere with the

336 normal tissues, resulting in damage to normal cells and other side effects.

337 Therefore, further toxicological experiments are needed to objectively evaluate the

338 application of targeted therapy in tumors with high SREBF1 expression.

339 Furthermore, analysis of the TCGA and UALCAN databases revealed that the

340 expression of SREBF1 was significantly higher in HNSC than in normal tissues. In

341 addition, high expression of SREBF1 correlated with tumor stage, lymph node

342 stage, and tumor grade in HNSC, suggesting that SREBF1 plays an important role

343 in the progression of HNSC.

344 To further investigate the role of SREBF1 in HNSC, enrichment analysis of related

345 genes showed that SREBF1 is associated with cell proliferation pathways such as

346 DNA replication and homologous recombination.

347 Further biological experiments indicated that the expression levels of SREBF1 and

348 STARD4 were significantly increased in HNSC cells. Knockdown of SREBF1

349 significantly inhibited the proliferation and migration of HNSC cell lines (Hep2

350 and TU212). The potential mechanisms underlying the role of SREBP1 in tumor

351 progression include promoting tumor growth by increasing lipid synthesis through

352 the activation of its target genes, as shown in prostate cancer, gastric cancer, and

353    bladder cancer (Du et al. 2012; Miyachi et al. 2013; Singh et al. 2019). In the

354    present study, the knockdown of SREBF1 in HNSC cells (Hep2 and TU212)

355    downregulated the expression of STARD4. High expression of STARD4 in breast

356    cancer has also been reported, and cell function experiments show that knockdown

357    of STARD4 significantly inhibits the proliferation and migration of breast cancer.

358    This suggests that SREBF1 may promote the proliferation and migration of head

359    and neck squamous cell carcinoma through STARD4. In this study, we showed

360    that SREBF1 is associated with the Fanconi anemia pathway, which is associated

361    with an increased risk of HNSC(Vigneswaran & Williams 2014). This supports the

362    potential association of SREBF1 with the development of HNSC and provides a

363    new theoretical basis for understanding the role of SREBF1 in promoting the

364    progression of HNSC.

365    Immune cells are an important component of the tumor microenvironment and play

366    an important role in regulating the malignant behavior of tumor cells (Binnewies et

367    al. 2018; Sahin Ozkan et al. 2020; Vilarino et al. 2020). Immune cell infiltration in

368    the tumor microenvironment is an important predictor of prognosis and treatment

369    outcome in cancer patients(Lee et al. 2017; Li et al. 2020a). Recent studies show

370    that tumor immune cell infiltration is associated with the prognosis of

371    HNSC(Zhang et al. 2020). However, whether SREBF1 expression is associated

372    with immune cell infiltration in HNSC remains unclear. We comprehensively

373    analyzed the correlation between SREBF1 expression and the level of immune cell

374 infiltration in HNSC. The results showed that the infiltration of    T helper cells and

375 NK CD56 bright cells was higher in the HNSC group with high SREBF1

376 expression than in the low expression group. Moreover, the expression of SREBF1

377 was significantly and positively correlated with the infiltration level of    T helper

378 cells and NK CD56 bright cells. Metabolic reprogramming supports the production

379 of IFN-γ by NK CD56 bright cells in the immune response(Keating et al. 2016),

380 and IFN-γ has immunomodulatory and antitumor effects. T helper cells are also

381 associated with immune responses in the tumor environment(Ostroumov et al.

382 2018). This suggests that SREBF1 is involved in regulating the HNSC immune

383 response.

384 ## 5. Conclusion

385 In conclusion, SREBF1 possibly through upregulation of STARD4 and affects

386 immune infiltration to promote proliferation, migration and inhibit apoptosis in

387 head and neck squamous cell carcinoma.

388

389 Funding: None

390 Additional Information and Declarations

391 Conflict of interest
392 The authors declare no conflict of interest.

393 Author Contributions

394   Ming Tan and Jiping Su: project development, data analysis, and validation, and manuscript

395   writing. Xiaoyu Lin,Huiying Chen,Wanli Ye,Chao Li,Jinlan Liu: sample collection. Ming Tan

396   and Jianqi Yi: manuscript editing. All authors read and approved the final manuscript.

397   Data Availability
398   The following information was supplied regarding data availability:
399   The raw data are available in the Supplemental File.

400

401

402

403

404   References

405   Ahmad Kiadaliri A, Jarl J, Gavriilidis G, and Gerdtham UG. 2013. Alcohol drinking cessation
406       and the risk of laryngeal and pharyngeal cancers: a systematic review and meta-analysis.
407       *PLoS One* 8:e58158. 10.1371/journal.pone.0058158
408   Bindea G, Mlecnik B, Tosolini M, Kirilovsky A, Waldner M, Obenauf AC, Angell H, Fredriksen
409       T, Lafontaine L, Berger A, Bruneval P, Fridman WH, Becker C, Pages F, Speicher MR,
410       Trajanoski Z, and Galon J. 2013. Spatiotemporal dynamics of intratumoral immune cells
411       reveal the immune landscape in human cancer. *Immunity* 39:782-795.
412       10.1016/j.immuni.2013.10.003
413   Binnewies M, Roberts EW, Kersten K, Chan V, Fearon DF, Merad M, Coussens LM,
414       Gabrilovich DI, Ostrand-Rosenberg S, Hedrick CC, Vonderheide RH, Pittet MJ, Jain RK,
415       Zou W, Howcroft TK, Woodhouse EC, Weinberg RA, and Krummel MF. 2018.
416       Understanding the tumor immune microenvironment (TIME) for effective therapy. *Nat*
417       *Med* 24:541-550. 10.1038/s41591-018-0014-x
418   Chen C, Guo Q, Song Y, Xu G, and Liu L. 2020. SKA1/2/3 serves as a biomarker for poor
419       prognosis in human lung adenocarcinoma. *Transl Lung Cancer Res* 9:218-231.
420       10.21037/tlcr.2020.01.20
421   Cheng C, Geng F, Cheng X, and Guo D. 2018. Lipid metabolism reprogramming and its
422       potential targets in cancer. *Cancer Commun (Lond)* 38:27. 10.1186/s40880-018-0301-4
423   Cheng C, Ru P, Geng F, Liu J, Yoo JY, Wu X, Cheng X, Euthine V, Hu P, Guo JY, Lefai E,
424       Kaur B, Nohturfft A, Ma J, Chakravarti A, and Guo D. 2015. Glucose-Mediated N-
425       glycosylation of SCAP Is Essential for SREBP-1 Activation and Tumor Growth. *Cancer*
426       *Cell* 28:569-581. 10.1016/j.ccell.2015.09.021
427   Cramer JD, Burtness B, Le QT, and Ferris RL. 2019. The changing therapeutic landscape of

428        head and neck cancer. *Nat Rev Clin Oncol* 16:669-683. 10.1038/s41571-019-0227-z

429    Du X, Wang QR, Chan E, Merchant M, Liu J, French D, Ashkenazi A, and Qing J. 2012. FGFR3
430        stimulates stearoyl CoA desaturase 1 activity to promote bladder tumor growth. *Cancer*
431        *Res* 72:5843-5855. 10.1158/0008-5472.CAN-12-1329

432    Fridman WH, Galon J, Dieu-Nosjean MC, Cremer I, Fisson S, Damotte D, Pages F, Tartour E,
433        and Sautes-Fridman C. 2011. Immune infiltration in human cancer: prognostic
434        significance and disease control. *Curr Top Microbiol Immunol* 344:1-24.
435        10.1007/82_2010_46

436    Gao Y, Nan X, Shi X, Mu X, Liu B, Zhu H, Yao B, Liu X, Yang T, Hu Y, and Liu S. 2019.
437        SREBP1 promotes the invasion of colorectal cancer accompanied upregulation of MMP7
438        expression and NF-kappaB pathway activation. *BMC Cancer* 19:685. 10.1186/s12885-
439        019-5904-x

440    Gholkar AA, Cheung K, Williams KJ, Lo YC, Hamideh SA, Nnebe C, Khuu C, Bensinger SJ,
441        and Torres JZ. 2016. Fatostatin Inhibits Cancer Cell Proliferation by Affecting Mitotic
442        Microtubule Spindle Assembly and Cell Division. *J Biol Chem* 291:17001-17008.
443        10.1074/jbc.C116.737346

444    Guo D, Bell EH, Mischel P, and Chakravarti A. 2014. Targeting SREBP-1-driven lipid
445        metabolism to treat cancer. *Curr Pharm Des* 20:2619-2626.
446        10.2174/13816128113199990486

447    Han J, Li E, Chen L, Zhang Y, Wei F, Liu J, Deng H, and Wang Y. 2015. The CREB coactivator
448        CRTC2 controls hepatic lipid metabolism by regulating SREBP1. *Nature* 524:243-246.
449        10.1038/nature14557

450    Hanzelmann S, Castelo R, and Guinney J. 2013. GSVA: gene set variation analysis for
451        microarray and RNA-seq data. *BMC Bioinformatics* 14:7. 10.1186/1471-2105-14-7

452    Huang CM, Huang CS, Hsu TN, Huang MS, Fong IH, Lee WH, and Liu SC. 2019. Disruption of
453        Cancer Metabolic SREBP1/miR-142-5p Suppresses Epithelial-Mesenchymal Transition
454        and Stemness in Esophageal Carcinoma. *Cells* 9. 10.3390/cells9010007

455    Jiang Y, Zhang Q, Hu Y, Li T, Yu J, Zhao L, Ye G, Deng H, Mou T, Cai S, Zhou Z, Liu H, Chen
456        G, Li G, and Qi X. 2018. ImmunoScore Signature: A Prognostic and Predictive Tool in
457        Gastric Cancer. *Ann Surg* 267:504-513. 10.1097/SLA.0000000000002116

458    Keating SE, Zaiatz-Bittencourt V, Loftus RM, Keane C, Brennan K, Finlay DK, and Gardiner
459        CM. 2016. Metabolic Reprogramming Supports IFN-gamma Production by CD56bright
460        NK Cells. *J Immunol* 196:2552-2560. 10.4049/jimmunol.1501783

461    Koizume S, Takahashi T, Yoshihara M, Nakamura Y, Ruf W, Takenaka K, Miyagi E, and
462        Miyagi Y. 2019. Cholesterol Starvation and Hypoxia Activate the FVII Gene via the
463        SREBP1-GILZ Pathway in Ovarian Cancer Cells to Produce Procoagulant Microvesicles.
464        *Thromb Haemost* 119:1058-1071. 10.1055/s-0039-1687876

465    Lee JM, Lee MH, Garon E, Goldman JW, Salehi-Rad R, Baratelli FE, Schaue D, Wang G, Rosen
466        F, Yanagawa J, Walser TC, Lin Y, Park SJ, Adams S, Marincola FM, Tumeh PC, Abtin F,
467        Suh R, Reckamp KL, Lee G, Wallace WD, Lee S, Zeng G, Elashoff DA, Sharma S, and
468        Dubinett SM. 2017. Phase I Trial of Intratumoral Injection of CCL21 Gene-Modified

469        Dendritic Cells in Lung Cancer Elicits Tumor-Specific Immune Responses and CD8(+)
470        T-cell Infiltration. *Clin Cancer Res* 23:4556-4568. 10.1158/1078-0432.CCR-16-2821

471  Li C, Jiang P, Wei S, Xu X, and Wang J. 2020a. Regulatory T cells in tumor microenvironment:
472        new mechanisms, potential therapeutic strategies and future prospects. *Mol Cancer*
473        19:116. 10.1186/s12943-020-01234-1

474  Li C, Peng X, Lv J, Zou H, Liu J, Zhang K, and Li Z. 2020b. SREBP1 as a potential biomarker
475        predicts levothyroxine efficacy of differentiated thyroid cancer. *Biomed Pharmacother*
476        123:109791. 10.1016/j.biopha.2019.109791

477  Li C, Yang W, Zhang J, Zheng X, Yao Y, Tu K, and Liu Q. 2014. SREBP-1 has a prognostic
478        role and contributes to invasion and metastasis in human hepatocellular carcinoma. *Int J*
479        *Mol Sci* 15:7124-7138. 10.3390/ijms15057124

480  Luo X, Cheng C, Tan Z, Li N, Tang M, Yang L, and Cao Y. 2017. Emerging roles of lipid
481        metabolism in cancer metastasis. *Mol Cancer* 16:76. 10.1186/s12943-017-0646-3

482  Ma X, Zhao T, Yan H, Guo K, Liu Z, Wei L, Lu W, Qiu C, and Jiang J. 2021. Fatostatin reverses
483        progesterone resistance by inhibiting the SREBP1-NF-kappaB pathway in endometrial
484        carcinoma. *Cell Death Dis* 12:544. 10.1038/s41419-021-03762-0

485  Marquard FE, and Jucker M. 2020. PI3K/AKT/mTOR signaling as a molecular target in head
486        and neck cancer. *Biochem Pharmacol* 172:113729. 10.1016/j.bcp.2019.113729

487  Meng H, Shen M, Li J, Zhang R, Li X, Zhao L, Huang G, and Liu J. 2021. Novel SREBP1
488        inhibitor cinobufotalin suppresses proliferation of hepatocellular carcinoma by targeting
489        lipogenesis. *Eur J Pharmacol* 906:174280. 10.1016/j.ejphar.2021.174280

490  Miyachi K, Sawada Y, Shida Y, Sugawara A, and Hisatomi H. 2013. Lipogenic gene expression
491        profile in patients with gastric cancer. *Mol Clin Oncol* 1:825-827. 10.3892/mco.2013.148

492  Ostroumov D, Fekete-Drimusz N, Saborowski M, Kuhnel F, and Woller N. 2018. CD4 and CD8
493        T lymphocyte interplay in controlling tumor growth. *Cell Mol Life Sci* 75:689-713.
494        10.1007/s00018-017-2686-7

495  Puram SV, Tirosh I, Parikh AS, Patel AP, Yizhak K, Gillespie S, Rodman C, Luo CL, Mroz EA,
496        Emerick KS, Deschler DG, Varvares MA, Mylvaganam R, Rozenblatt-Rosen O, Rocco
497        JW, Faquin WC, Lin DT, Regev A, and Bernstein BE. 2017. Single-Cell Transcriptomic
498        Analysis of Primary and Metastatic Tumor Ecosystems in Head and Neck Cancer. *Cell*
499        171:1611-1624 e1624. 10.1016/j.cell.2017.10.044

500  Rodriguez-Agudo D, Ren S, Wong E, Marques D, Redford K, Gil G, Hylemon P, and Pandak
501        WM. 2008. Intracellular cholesterol transporter StarD4 binds free cholesterol and
502        increases cholesteryl ester formation. *J Lipid Res* 49:1409-1419. 10.1194/jlr.M700537-
503        JLR200

504  Rohrig F, and Schulze A. 2016. The multifaceted roles of fatty acid synthesis in cancer. *Nat Rev*
505        *Cancer* 16:732-749. 10.1038/nrc.2016.89

506  Sahin Ozkan H, Ugurlu MU, Yumuk PF, and Kaya H. 2020. Prognostic Role of Immune
507        Markers in Triple Negative Breast Carcinoma. *Pathol Oncol Res* 26:2733-2745.
508        10.1007/s12253-020-00874-4

509  Schulze A, and Harris AL. 2012. How cancer metabolism is tuned for proliferation and

510  vulnerable to disruption. *Nature* 491:364-373. 10.1038/nature11706

511  Singh KB, Hahm ER, Pore SK, and Singh SV. 2019. Leelamine Is a Novel Lipogenesis Inhibitor
512      in Prostate Cancer Cells In Vitro and In Vivo. *Mol Cancer Ther* 18:1800-1810.
513      10.1158/1535-7163.MCT-19-0046

514  Thariat J, Vignot S, Lapierre A, Falk AT, Guigay J, Van Obberghen-Schilling E, and Milano G.
515      2015. Integrating genomics in head and neck cancer treatment: Promises and pitfalls. *Crit*
516      *Rev Oncol Hematol* 95:397-406. 10.1016/j.critrevonc.2015.03.005

517  Torre LA, Bray F, Siegel RL, Ferlay J, Lortet-Tieulent J, and Jemal A. 2015. Global cancer
518      statistics, 2012. *CA Cancer J Clin* 65:87-108. 10.3322/caac.21262

519  Tudek B, Zdzalik-Bielecka D, Tudek A, Kosicki K, Fabisiewicz A, and Speina E. 2017. Lipid
520      peroxidation in face of DNA damage, DNA repair and other cellular processes. *Free*
521      *Radic Biol Med* 107:77-89. 10.1016/j.freeradbiomed.2016.11.043

522  Vigneswaran N, and Williams MD. 2014. Epidemiologic trends in head and neck cancer and aids
523      in diagnosis. *Oral Maxillofac Surg Clin North Am* 26:123-141.
524      10.1016/j.coms.2014.01.001

525  Vilarino N, Bruna J, Bosch-Barrera J, Valiente M, and Nadal E. 2020. Immunotherapy in
526      NSCLC patients with brain metastases. Understanding brain tumor microenvironment
527      and dissecting outcomes from immune checkpoint blockade in the clinic. *Cancer Treat*
528      *Rev* 89:102067. 10.1016/j.ctrv.2020.102067

529  Wen YA, Xiong X, Zaytseva YY, Napier DL, Vallee E, Li AT, Wang C, Weiss HL, Evers BM,
530      and Gao T. 2018. Downregulation of SREBP inhibits tumor growth and initiation by
531      altering cellular metabolism in colon cancer. *Cell Death Dis* 9:265. 10.1038/s41419-018-
532      0330-6

533  Wu T, and Dai Y. 2017. Tumor microenvironment and therapeutic response. *Cancer Lett*
534      387:61-68. 10.1016/j.canlet.2016.01.043

535  Yang H, Zhang X, Liu F, Fan J, Wang B, and Dong C. 2018. SREBP1-driven lipid desaturation
536      supports clear cell renal cell carcinoma growth through regulation of NF-kappaB
537      signaling. *Biochem Biophys Res Commun* 495:1383-1388. 10.1016/j.bbrc.2017.11.163

538  Yang K, Zhang S, Zhang D, Tao Q, Zhang T, Liu G, Liu X, and Zhao T. 2019. Identification of
539      SERPINE1, PLAU and ACTA1 as biomarkers of head and neck squamous cell
540      carcinoma based on integrated bioinformatics analysis. *Int J Clin Oncol* 24:1030-1041.
541      10.1007/s10147-019-01435-9

542  Yi J, Zhu J, Wu J, Thompson CB, and Jiang X. 2020. Oncogenic activation of PI3K-AKT-
543      mTOR signaling suppresses ferroptosis via SREBP-mediated lipogenesis. *Proc Natl Acad*
544      *Sci U S A* 117:31189-31197. 10.1073/pnas.2017152117

545  Zeng D, Zhou R, Yu Y, Luo Y, Zhang J, Sun H, Bin J, Liao Y, Rao J, Zhang Y, and Liao W.
546      2018. Gene expression profiles for a prognostic immunoscore in gastric cancer. *Br J Surg*
547      105:1338-1348. 10.1002/bjs.10871

548  Zhang N, Zhang H, Liu Y, Su P, Zhang J, Wang X, Sun M, Chen B, Zhao W, Wang L, Wang H,
549      Moran MS, Haffty BG, and Yang Q. 2019. SREBP1, targeted by miR-18a-5p, modulates
550      epithelial-mesenchymal transition in breast cancer via forming a co-repressor complex

551      with Snail and HDAC1/2. *Cell Death Differ* 26:843-859. 10.1038/s41418-018-0158-8

552 Zhang X, Shi M, Chen T, and Zhang B. 2020. Characterization of the Immune Cell Infiltration

553      Landscape in Head and Neck Squamous Cell Carcinoma to Aid Immunotherapy. *Mol*

554      *Ther Nucleic Acids* 22:298-309. 10.1016/j.omtn.2020.08.030

555 Zhou C, Qian W, Li J, Ma J, Chen X, Jiang Z, Cheng L, Duan W, Wang Z, Wu Z, Ma Q, and Li

556      X. 2019. High glucose microenvironment accelerates tumor growth via SREBP1-

557      autophagy axis in pancreatic cancer. *J Exp Clin Cancer Res* 38:302. 10.1186/s13046-019-

558      1288-7

559 Zhou JP, Ren YD, Xu QY, Song Y, Zhou F, Chen MY, Liu JJ, Chen LG, and Pan JS. 2020.

560      Obesity-Induced Upregulation of ZBTB7A Promotes Lipid Accumulation through

561      SREBP1. *Biomed Res Int* 2020:4087928. 10.1155/2020/4087928

562

563

564

# Figure 1

SREBF1 expression in human pan-cancers.

(A) TCGA and GTEx databases provide information on SREBF1 expression in tumors and adjacent normal tissues, HNSC (Normal=44, Tumor=520). (B-C) Expression of SREBF1 and STARD4 in adjacent normal tissues and tumors in HNSC( Normal=44, Tumor=502) from unpaired samples in TCGA. (D-E) Expression of SREBF1and STARD4 in tumor and adjacent normal tissues in HNSC (Normal=43, Tumor=43) from paired samples in TCGA. TPM (transcripts per million reads), Data are shown as the mean ± SD. *P <0.05, **P < 0.01, ***P < 0.001.
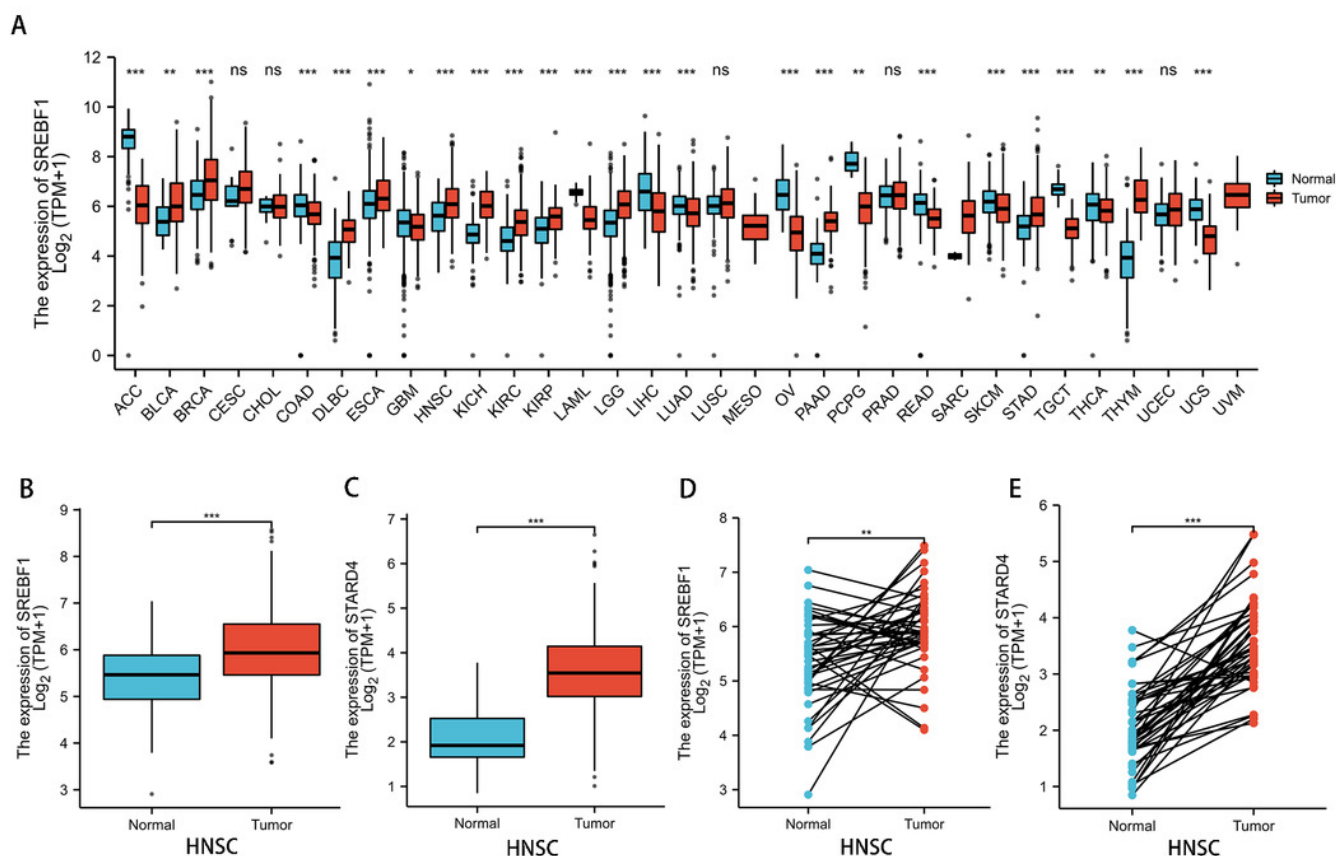
# Figure 2

Correlation of SREBF1 and STARD4 mRNA expression with clinicopathological parameters in HNSC patients from the UALCAN database.

(A+B)Type of sample (normal/primary tumor). (C+D)Cancer stage (stage1,2, 3,and4). (E+F)Lymph node stage (N0,1,2,and3). (G+H)Tumor grade (Grades1, 2, 3, and4). N, normal; P, primary tumor; S1, stage 1; S2, stage 2; S3, stage 3; S4, stage 4.G1, Grade1; G2, Grade2; G3, Grade3; G4, Grade4.
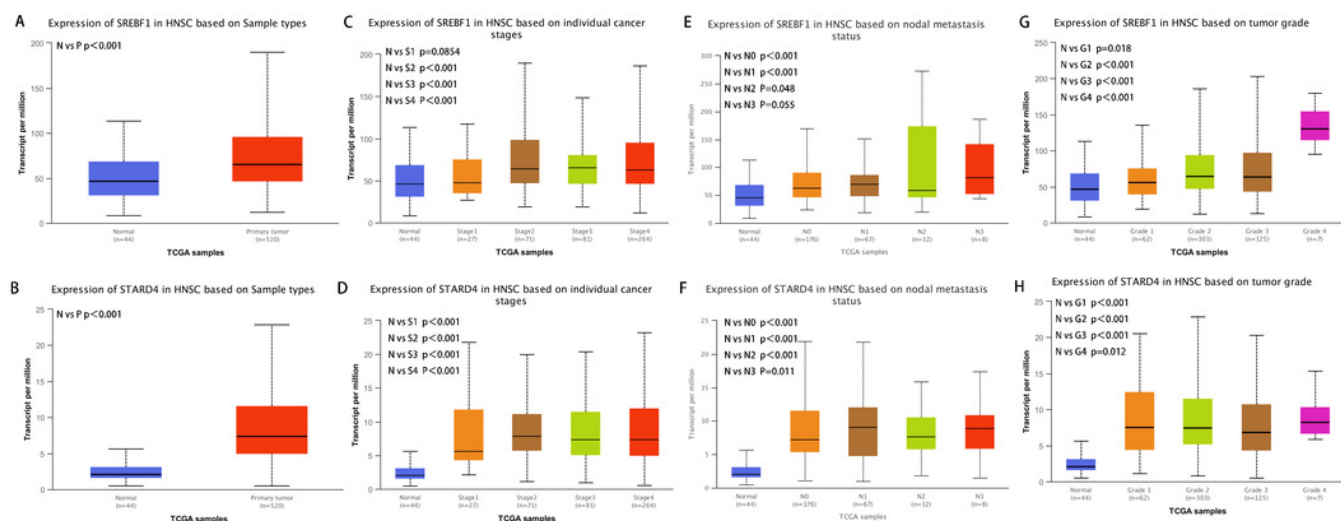
# Figure 3

Analysis of SREBF1-related genes.

The top 50 genes positively associated with SREBF1 expression are shown in the heat map.

The data were normalized by the Z-score normalization method.
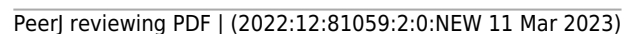
# Figure 4

Enrichment analysis of SREBF1-related genes in HNSC.

(A) KEGG pathways of genes significantly associated with SREBF1. (B-D) Gene ontology terms are significantly associated with SREBF1 [including biological processes (B), cell components (C), and molecular function (D)].
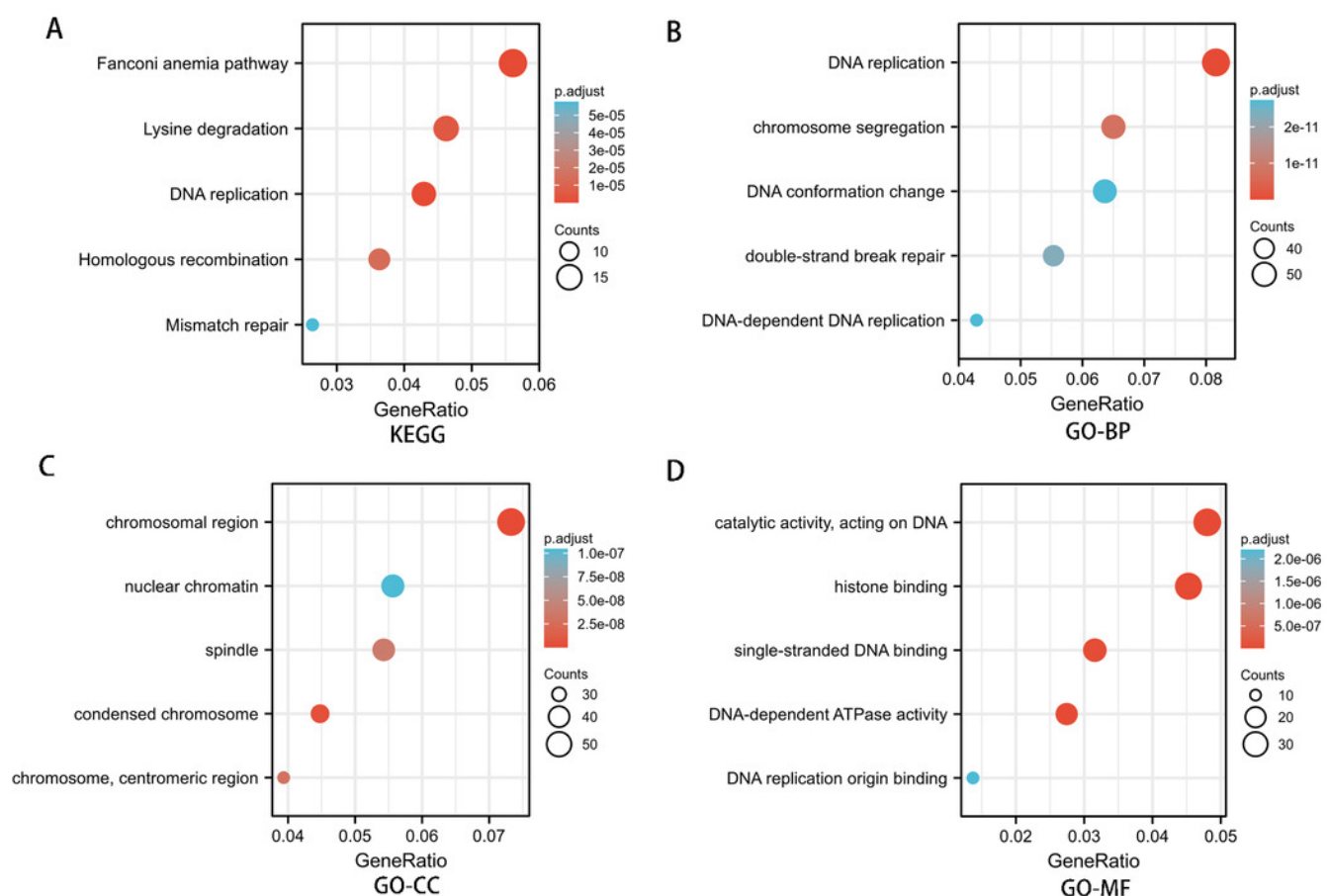
# Figure 5

SREBF1 expression and immune cell infiltration in HNSC are correlated.

(A) Comparison of immune cell infiltration levels between SREBF1 differentially expressed groups in TCGA cohort of HNSC. (B) Correlation between SREBF1 and immune cell infiltration levels; red represents a positive correlation, green represents a negative correlation, and color shades represent the strength of the correlation. The data are presented as the mean ± standard deviation. *P < 0.05, **P < 0.01, ***P < 0.001. ns, not significant.

A

B
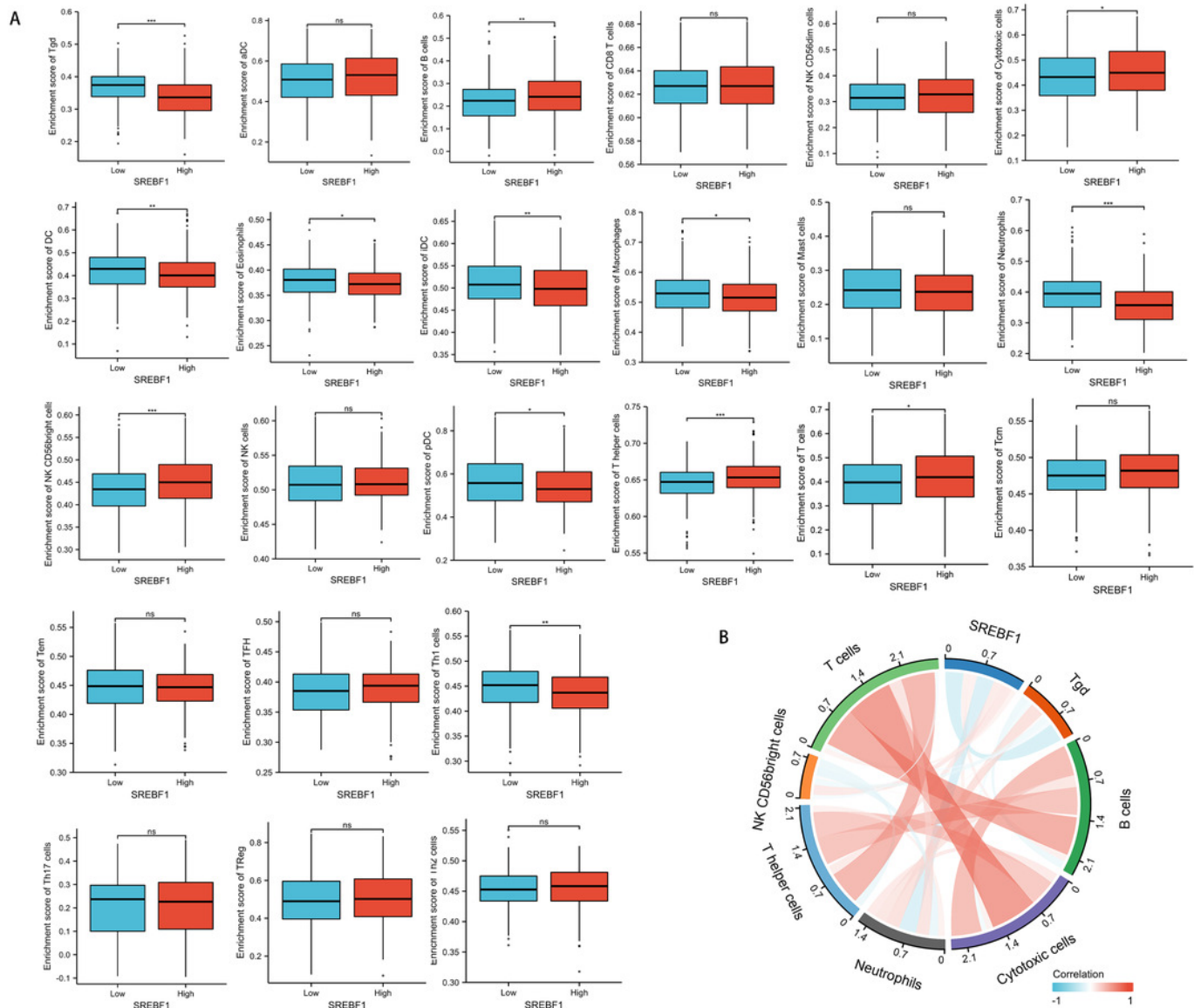
# Figure 6

Knockdown of SREBF1 inhibited the proliferation and migration of HNSC cells.

(A) Expression levels of SREBF1 mRNA and STARD4 mRNA were measured in HNSC cells by RT-qPCR. (B) SREBF1 was knocked down by RNA interference, and the levels of SREBF1 and STARD were assessed by RT-qPCR. (C) Western blot analysis of SREBF1 and STARD4 levels. (D-G) CCK-8 assay and flow cytometric assessment were used to detect HNSC cell growth. (H) A wound-healing assay was used to detect the capacity of HNSC cells to migrate (original magnification ×100). The data are presented as the mean ± SD. *P < 0.05, **P < 0.01, ***P < 0.001, ****P < 0.0001.